A quantitative kinetic model for Al$_2$O$_3$:C: TL response to ionizing radiation

V. Pagonis[a,*], R. Chen[b], J.L. Lawless[c]

[a]*Physics Department, McDaniel College, Westminster, MD21157, USA*
[b]*School of Physics and Astronomy, Raymond and Beverly Sackler Faculty of Exact Sciences, Tel-Aviv University, Tel-Aviv 69978, Israel*
[c]*Redwood Scientific Incorporated, Pacifica, CA, USA*

Abstract

This paper presents a quantitative kinetic model for the important dosimetric material Al$_2$O$_3$:C. The model consists of two traps and two centers, and reproduces the experimental thermoluminescence (TL) vs. dose behavior, as well as the experimental variation of the optical absorption coefficient K with beta dose. Initial estimates of the kinetic parameters in the model are obtained either from published experimental data, or by using reasonable physical assumptions. Good agreement between the experimental data and calculations from the model are obtained for three different types of samples of alumina. This is achieved by keeping the trapping and recombination probabilities constant for all three samples, while the concentrations of the carriers are varied. The kinetic model provides also a quantitative description of the experimentally observed nonmonotonic behavior of the TL dose–response curves for all three samples.
© 2006 Elsevier Ltd. All rights reserved.

Keywords: Thermoluminescence; Aluminum oxide; Kinetic model; Nonmonotonic dose behavior; Optical absorption; Thermoluminescence dosimetry

1. Introduction

The study of the thermoluminescence (TL) and optically stimulated luminescence (OSL) properties of Al$_2$O$_3$:C is of great practical importance for understanding the behavior of this important dosimetric material. There have been several previous attempts to produce theoretical models to describe various aspects of the response of this material to ionizing radiation (see, for example, Agersnap Larsen, 1999; Milman et al., 1998; Kortov et al., 1999; Kortov et al. 1999, 2006; McKeever, 2001 and references therein).

Yukihara et al. (2003) carried out a comprehensive experimental study of the effect of deep traps on the TL of Al$_2$O$_3$:C by using both beta irradiation and UV-illumination, as well as by employing step-annealing techniques. The concentrations of F- and F$^+$-centers in the samples were monitored by optical absorption measurements, and competing deep hole traps were identified which become unstable at 800–875 K, as well as competing electron traps which become unstable at 1100–1200 K.

These authors studied the TL dose–response and TL sensitivity and how these are affected by the filling of the deep hole and electron traps. Their study involved three samples from different batches labeled D320, Chip101 and B1040. Their data showed that the maximum height of the 450 K TL peak increased as a function of the beta dose up to $\sim$ 12–29 Gy for all three samples, and that at higher doses the TL signal decreased in the case of D320 and Chip101, while it reached a plateau at $\sim$ 600 Gy for B1040.

In the same series of experiments these authors also measured the optical absorption spectra after UV illumination, beta irradiation and step annealing of the samples. The absorption of the F$^+$-centers was used to study the dynamics of charge transfer during these three experiments, and the linear absorption coefficient K related to the F$^+$-centers was studied as a function of the beta dose. Samples D320 and Chip101 showed similar behaviors, exhibiting a decrease in the F$^+$ concentration for doses > 10 Gy up to beta doses of 100–200 Gy. Sample B1040 showed a distinctly different behavior with a peak shape of the optical absorption coefficient K around 100 Gy, a decrease between 100 and 1000 Gy, and an apparent increase for higher doses up to 2000 Gy.

---

* Corresponding author.

E-mail address: vpagonis@mcdaniel.edu (V. Pagonis).

Yukihara et al. (2003) concluded in their paper (p. 636), that the observed differences in sensitization, desensitization and TL dose–response between the three samples were due to (a) different concentrations of deep electron and deep hole traps and (b) due to different initial concentrations of the recombination centers (F^+-centers). This hypothesis by Yukihara et al. (2003) is verified by the simulations presented here.

The goal of this paper is to provide a mathematical description of the TL dose–response data and optical absorption experiments of Yukihara et al. (2003). The model presented here reproduces the experimental TL intensity vs. dose behavior for the three different samples termed D320, Chip101 and B1040, including the correct nonmonotonic behavior at high doses. The model also reproduces the corresponding experimental behavior of the optical absorption coefficient K as a function of beta dose. This is achieved by keeping the trapping and recombination probabilities constant for all three samples within the model, while the total and initial concentrations of the traps and centers are variable.

2. Recent theoretical modeling of the TL and OSL dose–response in alumina

The nonmonotonic dose dependence of TL has been observed in several materials. Chen et al. (2005) and Lawless et al. (2005) reviewed the experimental evidence in the literature and gave a theoretical description of this phenomenon as being the result of competition between transitions into different trapping states during the excitation stage, the read-out stage, or both.

Chen et al. (2006) and Pagonis et al. (2006) extended the work of Lawless et al. (2005) to the case of the nonmonotonic dose dependence of OSL. These authors gave several examples of kinetic models, which can reproduce the nonmonotonic OSL effect. Specifically, these authors used a model consisting of two trapping states and two kinds of recombination centers to explain the nonmonotonic dose dependence of the integrated OSL signal, and examined how the model can be applied to Al_2O_3:C. Chen et al. (2006) obtained both analytical and numerical results for the dose dependence of the integrated OSL and for the occupancies of the relevant traps and centers, and also for the relationship between these quantities and the constant equilibrium OSL values occurring at high doses in some samples.

Pagonis et al. (2006) obtained an estimate of the kinetic parameters for Al_2O_3:C by using a detailed series of physical arguments. Some of the parameters in the model are based on the experimental data of Yukihara et al. (2003), while other parameters are taken to represent "typical values" as reported in the literature for a variety of materials. Furthermore, an estimate was obtained for the conversion factor between the experimentally measured dose rate (in Gy/s), and the excitation rate X in the model (in electron–hole pairs per cm^3 per s), by using the physical properties of alumina. As a result of introducing this conversion factor, the experimental data can be shown on the same graph as the calculated curves of TL vs. dose and of K vs. dose. The doses given in these graphs are actually in Gy

and not in some arbitrary units, as is usually the practice in TL kinetic models.

In this paper we extend the work of Pagonis et al. (2006) to describe the experimentally observed nonmonotonic TL dose–response for the three alumina samples studied by Yukihara et al. (2003), termed D320, Chip101 and B1040.

3. The model

Yukihara et al. (2003) suggested in their Figure 10 a possible model to explain their extensive experimental results. Their suggested model consists of a composite main dosimetric trap, the deep hole trap, the deep electron trap and the F- and F^+-centers. Irradiation creates electron–hole pairs and the electrons are trapped either at the main dosimetric trap, or they recombine with the F^+-centers to create an F-center. The corresponding free holes created during irradiation are captured by the F-centers resulting in an increase in the concentration of F^+-centers. During heating of the samples, the electrons are freed from the main dosimetric trap and recombine with the F^+-centers creating an excited F-center, which leads to light emission with a wavelength of 420 nm.

The present model is a simplification of the model suggested by Yukihara et al. (2003), and consists of a single dosimetric trap, a competing deep electron trap, the radiative F^+-centers and the nonradiative deep hole centers. Fig. 1 shows in schematic form the transitions involved in the model. It is noted that the present model, the notation used here and the values of the kinetic parameters are identical to the ones used by Chen et al. (2006) to describe the nonmonotonic OSL dose dependence in alumina. The main features of the model and the relevant equations are repeated here for TL, for the sake of completeness.

The set of simultaneous differential equations governing the process during excitation with ionizing radiation

$$\frac{dm_1}{dt} = -A_{m1}m_1 n_c + B_1(M_1 - m_1)n_v, \tag{1}$$

$$\frac{dm_2}{dt} = -A_{m2}m_2 n_c + B_2(M_2 - m_2)n_v, \tag{2}$$

$$\frac{dn_1}{dt} = A_{n1}(N_1 - n_1)n_c, \tag{3}$$

$$\frac{dn_2}{dt} = A_{n2}(N_2 - n_2)n_c, \tag{4}$$

$$\frac{dn_c}{dt} = X - A_{m1}m_1 n_c - A_{m2}m_2 n_c$$
$$\quad - A_{n1}(N - n_1)n_c - A_{n2}(N - n_2)n_c, \tag{5}$$

$$\frac{dn_v}{dt} = X - B_2(M_2 - m_2)n_v - B_1(M_1 - m_1)n_v. \tag{6}$$

Here, as usual, M_1 (cm^{-3}) is the concentration of the radiative hole centers with instantaneous occupancy of m_1 (cm^{-3}), M_2 (cm^{-3}) is the concentration of nonradiative hole centers with instantaneous occupancy of m_2 (cm^{-3}), N_1 (cm^{-3}) is the concentration of the electron dosimetric trapping state
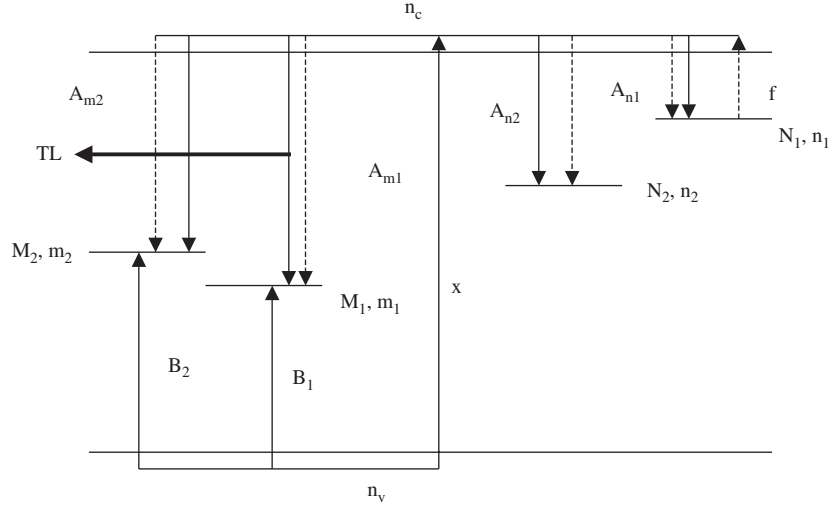
Fig. 1. The energy level diagram for the TL model in alumina, consisting of two trapping levels and two kinds of recombination centers. Transitions occurring during excitation are given by solid lines, and transitions taking place during the read-out stage are shown by dashed lines.

with instantaneous occupancy of n_1 (cm^{-3}), and N_2 (cm^{-3}) is the concentration of the deep electron trapping state with instantaneous occupancy of n_2 (cm^{-3}). n_c and n_v are the concentrations (cm^{-3}) of electrons and holes in the conduction and valence bands, respectively. X (cm^{-3} s^{-1}) is the rate of production of electron–hole pairs, which is proportional to the excitation dose rate, B_1 and B_2 (cm^3 s^{-1}) are the trapping coefficients of free holes in centers 1 and 2, respectively. A_{m1} and A_{m2} (cm^3 s^{-1}) are the recombination coefficients for free electrons with holes in centers 1 and 2 and A_{n1} (cm^3 s^{-1}) is the retrapping coefficient of free electrons into the dosimetric trapping state N_1. A_{n2} (cm^3 s^{-1}) is the retrapping coefficient of free electrons into the competing trapping state N_2.

If we denote the time of excitation by t_D and by X the rate of production electron–hole pairs per cm^3, then $X \cdot t_D$ represents the total concentration of electrons and holes produced, which is proportional to the total dose imparted. The units here are t_D in s and X in electron–hole pairs per cm^3 per s. In Pagonis et al. (2006), an estimate was obtained for the conversion factor between the experimentally measured dose rate (in Gy/s), and the excitation rate X (in electron–hole pairs per cm^3 per s) by using the physical properties of alumina. The value of X obtained in this previous work is used also throughout this simulation and is equal to:

$$X = 1.7 \times 10^{15} \text{ electron–hole pairs per cm}^3 \text{ per s}$$

$$= 1\,\text{Gy/s}. \tag{7}$$

As usual in TL kinetic models, a relaxation time of 60 s is simulated following the excitation and prior to the heating stage, during which practically all the free carriers relax and end up in the traps and centers. The simulation of the relaxation period is followed by the heating stage during which a linear heating function $T = T_0 + \beta t$ is used, where β is the constant heating rate. In our simulation the linear heating rate $\beta = 1\,\text{K}\,\text{s}^{-1}$. The

equations to be solved during the heating stage are

$$\frac{dm_1}{dt} = -A_{m1} m_1 n_c, \tag{8}$$

$$\frac{dm_2}{dt} = -A_{m2} m_2 n_c, \tag{9}$$

$$\frac{dn_1}{dt} = -n_1 s e^{-E/kT} + A_{n1}(N_1 - n_1)n_c, \tag{10}$$

$$\frac{dn_2}{dt} = A_{n2}(N_2 - n_2)n_c, \tag{11}$$

$$\frac{dn_1}{dt} + \frac{dn_2}{dt} + \frac{dn_c}{dt} = \frac{dm_1}{dt} + \frac{dm_2}{dt}. \tag{12}$$

Here E (eV) is the activation energy for the dosimetric trap, and s (s^{-1}) is the corresponding frequency factor. The TL intensity $I(T)$ is associated with the electron–hole recombination in the luminescence center m_1, therefore it is given by:

$$I(T) = A_{m1} m_1 n_c \eta(T). \tag{13}$$

Here the temperature-dependent factor $\eta(T)$ describes the thermal quenching of the TL intensity (see, for example, Bailey, 2001). This thermal quenching efficiency is given by

$$\eta(T) = \frac{1}{1 + C_1 \exp(-W_1/kT)}, \tag{14}$$

where the thermal quenching constants $W_1 = 1.1\,\text{eV}$ and $C_1 = 10^{11}$, as obtained from several previous experimental studies of thermal quenching effects in this material (see, for example, Akselrod et al., 1998; Agersnap Larsen, 1999; Kitis, 2002 and references therein).

The first column of Table 1 shows the kinetic parameters for sample Chip101 obtained by Pagonis et al. (2006) by using published experimental data and several physical arguments. The ultimate success of the model will be judged by how well it can fit the experimental data, so the initial estimates of the

Table 1
The parameters used in the simulation for the three samples

	D320	Chip101	B1040
M_1 (cm^{-3})	10^{17}	10^{17}	10^{17}
B_1 (cm^3 s^{-1})	10^{-8}	10^{-8}	10^{-8}
A_{m1} (cm^3 s^{-1})	4×10^{-8}	4×10^{-8}	4×10^{-8}
M_2 (cm^{-3})	2.3×10^{16}	2.4×10^{16}	2.5×10^{17}
B_2 (cm^3 s^{-1})	4×10^{-9}	4×10^{-9}	4×10^{-9}
A_{m2} (cm^3 s^{-1})	5×10^{-11}	5×10^{-11}	5×10^{-11}
N_1 (cm^{-3})	2×10^{15}	2×10^{15}	1.7×10^{17}
A_{n1} (cm^3 s^{-1})	2×10^{-8}	2×10^{-8}	2×10^{-8}
N_2 (cm^{-3})	0.4×10^{15}	2×10^{15}	10^{17}
A_{n2} (cm^3 s^{-1})	2×10^{-9}	2×10^{-9}	2×10^{-9}
m_{10} (cm^{-3})	1.75×10^{16}	9.4×10^{15}	0

(a)

(a)

(b)

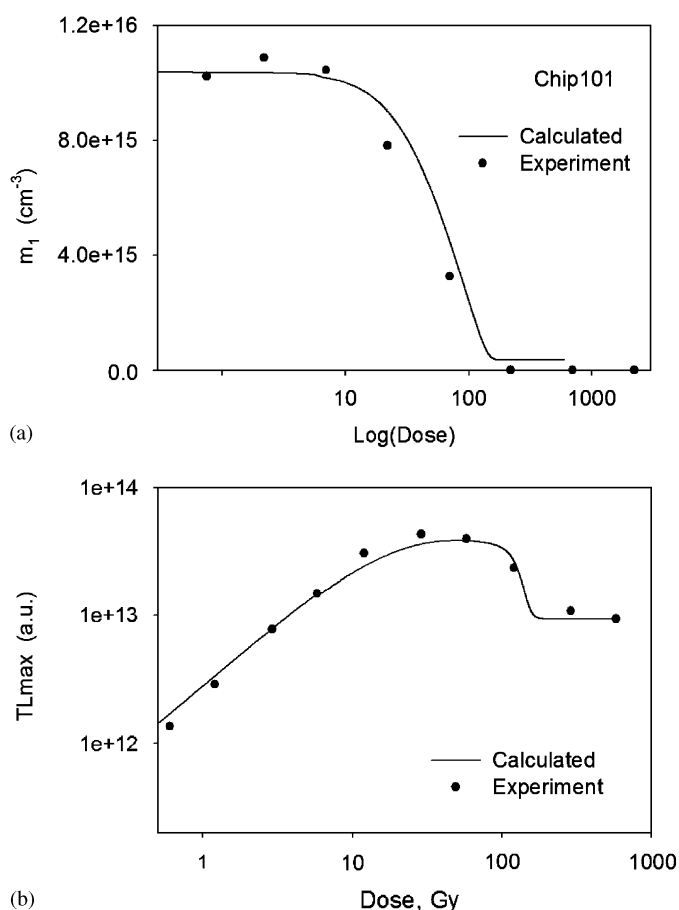Fig. 3. Same as Fig. 2, for sample D320.

(b)

Fig. 2. Comparison of calculations from the model (solid lines) and the experimental data of Yukihara et al. (2003). (a) The concentrations of luminescence centers m_1 as a function of the beta dose, and (b) the TL dose–response curves as a function of the beta dose, for sample Chip101. The kinetic parameters used are shown in Table 1. The experimental data for (a) is the absorption coefficient K (cm^{-1}) vs. beta dose shown in Fig. 8a of Yukihara et al. (2003), while the data for (b) are shown in their Fig. 2a.

parameters were adjusted to give as good a fit as possible to the data of Yukihara et al. (2003). Two additional sets of adjusted parameters are given in Table 1, for samples D320 and B1040. These three sets of parameters produce the theoretical curves shown in Figs. 2–4.
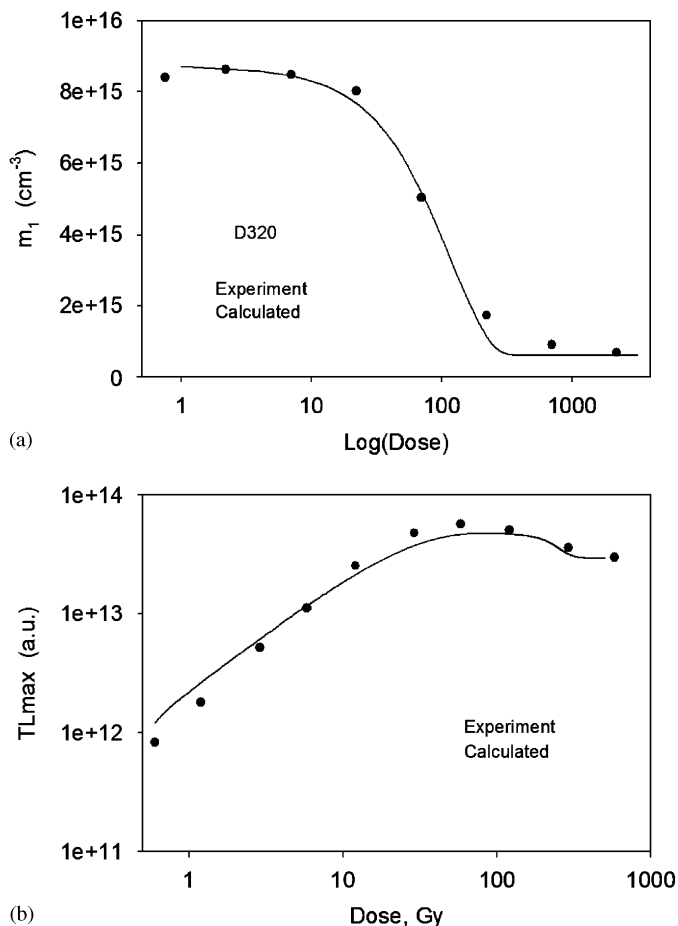
Of particular importance in the model are the initial occupancies of the luminescence centers (m_{10}) for each of the three samples studied. The experimental data of Yukihara et al. (2003, Figure 8a), show that at low beta doses, the optical absorption coefficient K (cm^{-1}), and correspondingly the concentration of the recombination centers m_1, stay approximately constant. This observation leads to a mathematical condition that must be satisfied by the kinetic parameters, so that the initial slope of the graph of m_1 vs. dose is zero ($\mathrm{d}m_1/\mathrm{d}D \sim 0$). This condition was used in Pagonis et al. (2006) to obtain an estimate of the initial concentration m_{10} of the carriers in the radiative center. It is noted that the data of Fig. 8a in Yukihara et al. (2003) show an important difference between the behavior of samples D320 and Chip101 on one hand, and that of sample B1040 on the other. The optical absorption coefficient K for sample B1040 in Fig. 8a of Yukihara et al. (2003) has a value of practically zero, indicating that the initial concentration of recombination centers $m_{10} \sim 0$ for this sample. At the same time Figure 8a shows that sample D320 has the highest K value at low doses of $K \sim 1.1\,\mathrm{cm}^{-1}$, while Chip101 has a value of $K \sim 0.45\,\mathrm{cm}^{-1}$ at low beta doses. These experimental values are consistent with the values of m_{10} shown in Table 1 for the three samples. The initial values of the remaining concentrations in the simulation are taken as $n_c = n_v = n_1 = n_2 = m_2 = 0$.
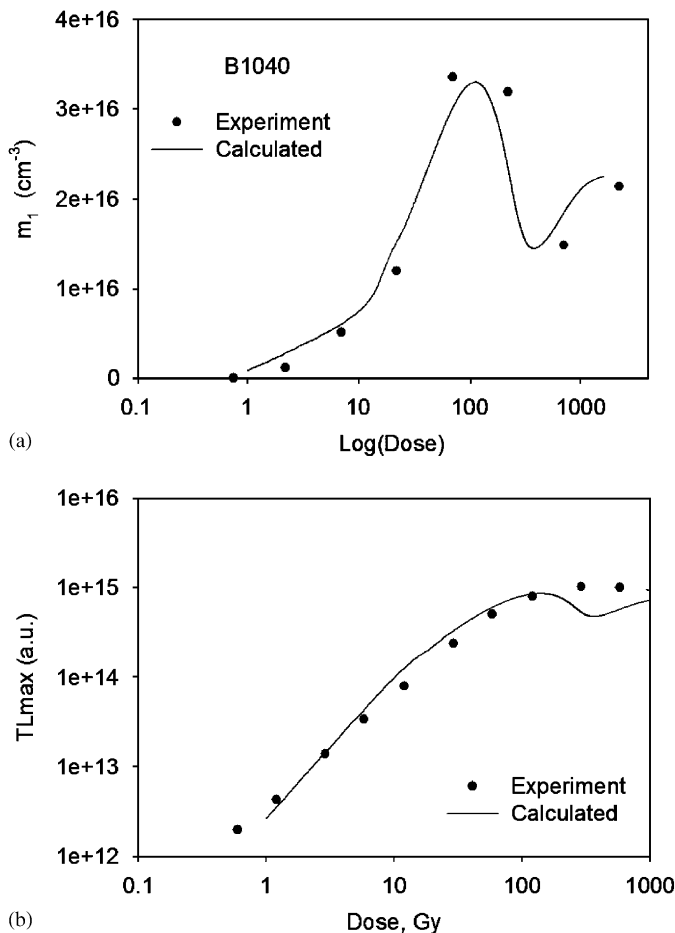
(a)

(b)

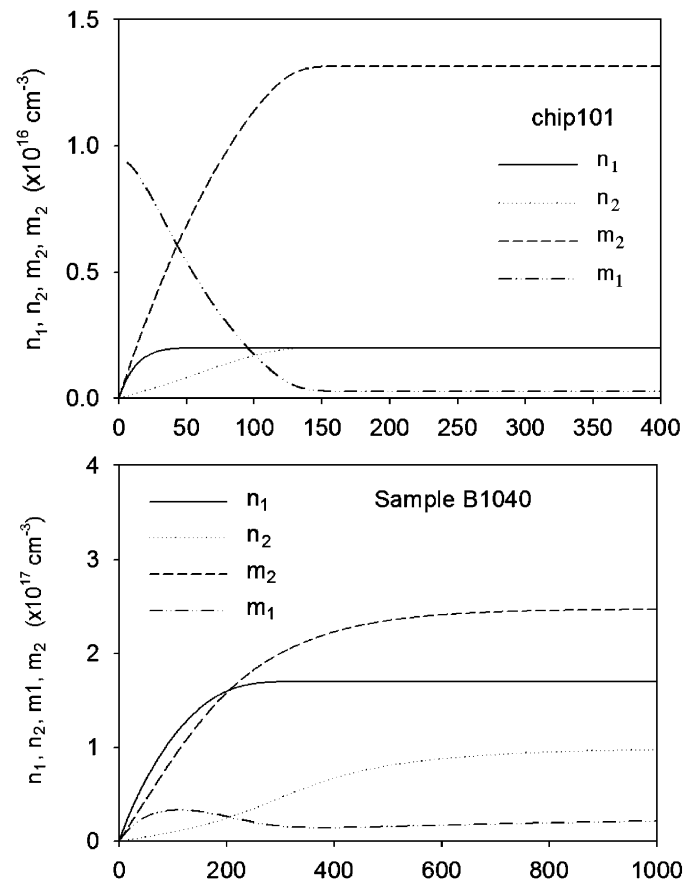Fig. 4. Same as Fig. 2, for sample B1040.

Fig. 5. The electron and hole concentrations at the end of the relaxation after the irradiation stage, as calculated from the model, as a function of the beta dose, for (a) sample Chip101 and (b) sample B1040.

The values of the parameters in Table 1 show that the different behaviors of the samples D320, Chip101 and B1040 can be explained by differences in the concentrations N_1, N_2, M_1, M_2 and m_{10} in the model, while the retrapping and recombination probability parameters are the same for the three samples.

The Mathematica differential equation solver, as well as the Matlab odes23 solver were used to solve numerically the relevant sets of equations; the results reached by these two solvers were in very good agreement.

4. Numerical results

Figs. 2–4 show the results of running the program with the parameters in Table 1. The solid lines in these figures represent the calculated dependence of the TL signal and of the occupancy of luminescence centers (m_1) on the excitation dose. The TL signal is defined here and in the Yukihara data as the maximum TL intensity. The experimental data of Yukihara et al. (2003) are also shown in Figs. 2–4. The y-axis of the experimental data has been multiplied by a scaling factor for comparison purposes, while no scaling has been applied to the dose axis. Figs. 2–4 show good agreement between theory and experiment, with the nonmonotonic effect of the appropriate magnitude appearing at the correct experimental dose.

The calculated TL dose–response curves for samples Chip101 and D320 in Figs. 2b and 3b reach a broad maximum at about 30 Gy and subsequently decrease at higher doses, showing nonmonotonic dose dependence. On the other hand, the corresponding calculated curve in Fig. 4b for sample B1040 reaches a plateau at ~ 600 Gy. The calculated m_1 vs. dose curves in Figs. 2a and 3a for samples D320 and Chip101 showed a similar behavior, exhibiting a decrease for doses > 10 Gy up to beta doses of 100–200 Gy. The corresponding calculated curve in Fig. 4a for sample B1040 shows a distinct peak shape around 100 Gy, a decrease between 100 and 1000 Gy, and an increase for higher doses up to 2000 Gy.

Fig. 5a and b shows the detailed behavior of the concentrations of holes and electrons in samples Chip101 and B1040 at the end of the relaxation period. The behavior of sample D320 is very similar to that of sample Chip101 and is not shown here.

The calculated curves in Fig. 5a for sample Chip101 show that the dosimetric peak saturates at ~ 30 Gy, while the deep electron trap saturates at a higher dose of ~ 120 Gy. The deep hole trap (m_2) reaches equilibrium at about ~ 150 Gy. The physical basis of the nonmonotonic TL effect in alumina according to the present model is the same as for the corresponding nonmonotonic OSL effect, which has been discussed in detail in Chen et al. (2006). The relevant OSL simulations

and the detailed discussion for Chip101 (and for the similar sample D320) can be found in Figs. 2 and 3 and on pp. 4–5 of that paper, and will not be repeated here.

The calculated curves in Fig. 5b for sample B1040 show that the dosimetric peak saturates at $\sim 100\,$Gy, while the deep electron trap saturates at a higher dose of $\sim 600\,$Gy. The deep hole trap (m_2) reaches equilibrium at $\sim 600\,$Gy. The critical factor that causes a different behavior in this sample is the initial nil concentration of luminescence centers $m_{10} \sim 0$. The behavior of the nonmonotonic OSL effect in this type of sample was also studied in Figs. 4 and 5 and on pp. 4–6 of the paper by Chen et al. (2006). The physical arguments are identical in the case of the nonmonotonic effect in TL.

The above explanations of the nonmonotonic TL effect in alumina are in agreement with the theoretical study by Lawless et al. (2005), who showed that this commonly observed nonmonotonic behavior of TL dose–response curves can be explained on the basis of processes involving either competition during irradiation, or by competition during the heating stage of TL experiments, or both.

As a further check, the model reproduces the correct qualitative dose dependence of the temperature of maximum experimental TL intensity (T_{max}). As the beta dose increases, the experimental TL glow curves shift towards lower temperatures. Specifically for sample Chip101, the experimental data of Yukihara et al. (2003) show that the value of T_{max} stays approximately the same at $\sim 190\,°$C for doses up to $\sim 10\,$Gy, while it steadily declines for higher doses down to a value of $\sim 165\,°$C for a dose of $\sim 300\,$Gy. The behavior of T_{max} vs. dose is very similar for sample D320, with an initial value of $\sim 190\,°$C for doses $< 10\,$Gy, and a steady decline to a value of $170\,°$C for large dose of $\sim 500\,$Gy. Once more, sample B1040 exhibits a very different behavior with T_{max} increasing steadily from a value of ~ 184 to a value of $200\,°$C in the range 0.6–10 Gy, and with a steady subsequent decline down to $\sim 175\,°$C for a large dose of $\sim 600\,$Gy. The model reproduces well this experimental T_{max} vs. dose behavior for sample Chip101, within $\sim 5\,$K. The agreement for samples D320 and B1040 is not as good quantitatively, but the simulation displays the same general qualitative behavior as the experimental data.

The simplified model used here also produces the correct first-order shape for the TL glow curves, but does not reproduce the experimental glow curve widths. For example, in the case of sample Chip101, the simulation shows an increase in the FWHM of the glow curves from 35 to 40 K in the dose interval 0.6–90 Gy, and a subsequent decrease to a value of $\sim 30\,$K for doses in the interval 90–300 Gy; the experimental data of Yukihara et al. (2003) indicate much wider glow peaks with FWHM values of ~ 45–52 K between 0.6 and 600 Gy.

This discrepancy between the model used here and the experimental data can be easily understood on the basis of additional experimental data available in the literature for this material. Previous experimental studies have shown that the dosimetric peak at 450 K has a composite structure, which has been interpreted as either involving two components corresponding to the release of both electrons and holes from the traps, or as a series of overlapping first-order TL peaks (Agersnap Larsen, 1999;

Agersnap Larsen et al., 1999; Colyott et al., 1996; Whitley and McKeever, 2000). Furthermore, the observed widths of the TL glow curves are affected by the finite thickness (0.9 mm) of the samples used by Yukihara et al. (2003), especially at high doses. The irradiated front of the crystals will be receiving higher effective doses during irradiation, with the dose getting smaller towards the back of the samples, and this impacts both the TL glow curves and the shape of the OSL decay curves for alumina (see, for example, Yukihara et al., 2004a, b).

5. Conclusions

The work presented in this paper extends the recent work of Chen et al. (2006) and Pagonis et al. (2006) on the nonmonotonic behavior of OSL vs. dose, to the corresponding nonmonotonic TL behavior of alumina. The results show that the same kinetic parameters can provide a quantitative description of the experimentally observed nonmonotonic effect for both OSL and TL in Al_2O_3:C.

Al_2O_3:C is an unusual dosimetric material, in the sense that we know the nature of the recombination centers, and therefore optical measurements can be used to study the m_1 vs. dose and m_1 vs. annealing temperature behaviors, in addition to the usual TL vs. dose response. The quantitative model presented in this paper produces good agreement with the available experimental data for TL vs. beta dose and m_1 vs. beta dose curves, and for three different types of samples. Within the model the concentrations M_1, M_2, N_1 and N_2 are allowed to vary for the different samples and the rest of the kinetic constants are kept constant, in agreement with the conclusions of Yukihara et al. (2003).

Preliminary results show that the same model can also provide a quantitative description of the TL vs. UV-fluence and m_1 vs. UV-fluence dependencies for this material.

It must be noted that a different theoretical approach has been presented recently by Kortov et al. (2006) for anion-defect α-Al_2O_3 single crystals. These authors investigated the mechanism of formation of nonlinearity in the dose dependence of the TL output. Their experimental work showed that the nonlinearity of the dose dependence of the TL output depends on the heating rate used during measurement of TL. This effect was explained within a comprehensive framework of the interaction between the dosimetric and deep traps.

A more comprehensive model for this material must include: (a) the known shallow TL traps, (b) thermal dissociation of deep hole traps and deep electron traps at appropriate temperatures, and (c) localized transitions between F and F^+-centers and (d) the effect of finite thickness of the sample.

References

Agersnap Larsen, N., 1999. Dosimetry based on thermally and optically stimulated luminescence. Ph.D. Thesis, Riso National Laboratory, Roskilde, Denmark. Available online at ⟨ http://www.risoe.dk/rispubl/NUK/ris-r-1090.htm ⟩.

Agersnap Larsen, N., Botter-Jensen, L., McKeever, S.W.S., 1999. Thermally stimulated conductivity and thermoluminescence from Al$_2$O$_3$:C. Radiat. Prot. Dosim. 84, 87–90.

Akselrod, M.S., Agersnap Larsen, N., Whitley, V., McKeever, S.W.S., 1998. Thermal quenching of F-center luminescence in Al$_2$O$_3$:C. J. Appl. Phys. 84, 3364–3373.

Bailey, R.M., 2001. Towards a general kinetic model for optically and thermally stimulated luminescence of quartz. Radiat. Meas. 33, 17–45.

Chen, R., Lo, D., Lawless, J.L., 2006. Non-monotonic dose dependence of thermoluminescence. Radiat. Prot. Dosim., in press, doi: 10.1093/rpd/nci599.

Chen, R., Pagonis, V., Lawless, J.L., 2006. The nonmonotonic dose dependence of optically stimulated luminescence in Al$_2$O$_3$:C: analytical and numerical simulation results. J. Appl. Phys. 99, 033511.

Colyott, L.E., Akselrod, M.S., McKeever, S.W.S., 1996. Phototransferred thermoluminescence in α-Al$_2$O$_3$:C. Radiat. Prot. Dosim. 65, 263–266.

Kitis, G., 2002. Confirmation of the influence of thermal quenching on the initial rise method in α-Al$_2$O$_3$:C. Phys. Status Solidi (A), Appl. Res. 191 (2), 621–627.

Kortov, V.S., Milman, I.I., Nikiforov, S.V., 1999. The effect of deep traps on the main features of thermoluminescence in dosimetric α-Al$_2$O$_3$ crystals. Radiat. Prot. Dosim. 84, 35–38.

Kortov, V.S., Milman, I.I., Nikiforov, S.V., Moiseĭkin, E.V., 2006. Mechanism of formation of nonlinearity in the dose dependence of the thermoluminescence output for anion-defect α-Al$_2$O$_3$ crystals. Phys. Solid State 48 (3), 447–452.

Lawless, J.L., Chen, R., Lo, D., Pagonis, V., 2005. A model for non-monotonic dose dependence of thermoluminescence. J. Phys.: Condens. Matter 17, 737–753.

McKeever, S.W.S., 2001. Optically stimulated luminescence dosimetry. Nucl. Instr. Methods Phys. Res. B 184, 29–54.

Milman, I.I., Kortov, V.S., Nikiforov, S.V., 1998. An interactive process in the mechanism of the thermally stimulated luminescence of anion-defective α-Al$_2$O$_3$ crystals. Radiat. Meas. 29, 401–410.

Pagonis, V., Chen, R., Lawless, J.L., 2006. Non-monotonic dose dependence of OSL intensity due to competition during irradiation and read-out, Radiat. Meas., in press, doi: 10.1016/j.radmeas.2006.04.002.

Whitley, V.H., McKeever, S.W.S., 2000. Photoionization of deep centers in Al$_2$O$_3$. J. Appl. Phys. 87, 249–256.

Yukihara, E.G., Whitley, V.H., Polf, J.C., Klein, D.M., McKeever, S.W.S., Akselrod, A.E., Akselrod, M.S., 2003. The effects of deep trap population on the thermoluminescence of Al$_2$O$_3$:C. Radiat. Meas. 37, 627–638.

Yukihara, E.G., Whitley, V.H., McKeever, S.W.S., Akselrod, A.E., Akselrod, M.S., 2004a. Effect of high-dose irradiation on the optically stimulated luminescence of Al$_2$O$_3$:C. Radiat. Meas. 38, 317–330.

Yukihara, E.G., Gaza, R., McKeever, S.W.S., Soares, C.G., 2004b. Optically stimulated luminescence and thermoluminescence efficiencies for high-energy heavy charged particle irradiation in Al$_2$O$_3$:C. Radiat. Meas. 38, 59–70.